

# Experimental investigation of optical atom traps with a frequency jump

P Ahmadi, G Behinaein, B P Timmons and G S Summy

*Department of Physics, Oklahoma State University, Stillwater, Oklahoma 74078-3072*

## Abstract

We study the evolution of a trapped atomic cloud subject to a trapping frequency jump for two cases: stationary and moving center of mass. In the first case, the frequency jump initiates oscillations in the cloud's momentum and size. At certain times we find the temperature is significantly reduced. When the oscillation amplitude becomes large enough, local density increases induced by the anharmonicity of the trapping potential are observed. In the second case, the oscillations are coupled to the center of mass motion through the anharmonicity of the potential. This induces oscillations with even larger amplitudes, enhancing the temperature reduction effects and leading to nonisotropic expansion rates while expanding freely.

PACS numbers: 32.80.Lg, 32.80.Pj

## I. INTRODUCTION

A trapped atomic cloud subjected to a sudden change in its trapping potential can exhibit a wide range of behavior with many possible applications. It can be used as a model for studying fundamental phenomenon ranging from superfluidity to the generation of non-classical states of a matter-wavepacket. For instance, a Bose-Einstein condensate can be reversibly created by suddenly changing the trapping potential [1]; sinusoidally moving a magnetic trap center can be used to observe the excitation modes of a Bose-Einstein condensate [2]; the modulation of optical traps can be used for coherent control of the center of mass wavepacket [3]; and the breathing mode oscillation of atomic clouds in 1D and 3D optical lattices can be realized by suddenly changing the lattice depth [4]. The latter has also captured a great deal of theoretical interest because of the possibility of creating squeezed states of a matter wavepacket [5, 6, 7, 8, 9, 10, 11].

The oscillation of an atomic cloud after a sudden jump in the trapping frequency has also been proposed as a tool for optical cooling and hence controlling the onset of Bose-Einstein condensation [12, 13]. This cooling method can be categorized among the techniques that use geometrical manipulation of an external potential to reduce the temperature of atoms or molecules. For example, Flories *et al.* [14] used a spatially varying electric field to longitudinally cool a molecular beam to 250 nK, while Ketterle and coworkers achieved pico-Kelvin temperatures by adiabatically decompressing a gravito-magnetic trap [15]. Exposing a freely expanding cloud of cold atoms to a pulsed potential has also been considered as a method for temperature reduction [16].

In this paper we use optical traps to experimentally realize a potential with a sudden frequency jump so as to explore the cooling proposals of Ref. [12]. These traps have become versatile tools for atom optics research, with the observation of all-optical Bose-Einstein condensation an example of their dramatic potential [17]. Early experiments on intensity modulation of the laser beam used to form an optical trap [4, 18, 19, 20] were used to demonstrate the parametric excitation of an atomic cloud. In this paper we will discuss experiments with these traps, comparing the observations with theory, and presenting possible future applications. The format of this paper is as follows. In Section II the experimental configuration is reviewed. In Section III we first lay out the theory of non-adiabatic cooling of an atomic cloud, then follow by presenting experimental data for the

case of a sudden frequency jump with a stationary center of mass. This discussion is then repeated in Section IV for the case of a moving center of mass.

## II. EXPERIMENTAL CONFIGURATION

Our experimental apparatus has been described previously [21, 22] so only a brief description is given here. We create a potential for Rb87 atoms using their interaction with 10.6  $\mu\text{m}$  light from a CO<sub>2</sub> laser. The CO<sub>2</sub> laser radiation frequency is far enough below that of the resonances of the atoms that its electric field can be considered quasi-static. This induces a dipole moment proportional to the local electric field and a lowering of the atomic ground state energy given by,  $U = -\frac{1}{2}\alpha_g|E|^2$ , where  $\alpha_g$  is the ground state static polarizability and  $|E|^2$  is the time averaged square of the laser light's electric field.

Two CO<sub>2</sub> beams were directed into a vacuum chamber in a geometry such that they propagated orthogonally to each other. One of the beams propagated in the vertical direction ( $x$  direction) and the other in the horizontal direction ( $z$  direction). Crucially the position where the  $x$  beam intersected the  $z$  beam could be adjusted. That is, the foci of the two beams did not necessarily coincide. The light for these beams originated from a 50 Watt RF excited CO<sub>2</sub> laser whose total power was controlled by passing the output light through an acousto-optic modulator (AOM). The first order beam of the modulator was then directed into another AOM which was used as a beamsplitter whose ratio could be changed by varying the input RF power. This ratio was used to control the time dependent potential. In order to fulfill the conditions necessary for this experiment, the CO<sub>2</sub> beams were aligned such that the  $x$  beam was the first order of the second AOM and the  $z$  beam the zeroth order of the same AOM. The data were taken by destructively imaging the cloud using a resonant probe laser which passed through the atom cloud and was then incident on a CCD camera. A gaussian fit to the optical density data determined the spatial extent of the atomic cloud.

## III. STATIONARY CENTER OF MASS

We begin by theoretically considering the situation where the center of mass of the atomic cloud remains stationary after a sudden change in the trapping potential. We take a sample of atoms in thermal equilibrium inside a harmonic potential of frequency  $\omega_0$  which is non-

adiabatically changed to  $\omega_1$  at  $t = 0$ . Neglecting the effect of collisions and following Balatov *et al.* [12], the momentum and position probability distribution widths are given by,

$$\sigma_p^2(t) = \frac{1}{2}\sigma_p^2(0)[1 + (\frac{\omega_1}{\omega_0})^2 + (1 - (\frac{\omega_1}{\omega_0})^2) \cos(2\omega_1 t)] \quad (1)$$

$$\sigma_z^2(t) = \frac{1}{2}\sigma_z^2(0)[1 + (\frac{\omega_0}{\omega_1})^2 + (1 - (\frac{\omega_0}{\omega_1})^2) \cos(2\omega_1 t)] \quad (2)$$

where at  $t = \frac{\pi}{2\omega_1}$  they reduce to,

$$\sigma_p^2(\frac{\pi}{2\omega_1}) = (\frac{\omega_1}{\omega_0})^2 \sigma_p^2(0) \quad (3)$$

$$\sigma_z^2(\frac{\pi}{2\omega_1}) = (\frac{\omega_0}{\omega_1})^2 \sigma_z^2(0). \quad (4)$$

For  $\omega_1 \ll \omega_0$ , a narrow momentum distribution is produced corresponding to a lower effective temperature. In the case of a single Gaussian laser beam propagating in the  $z$  direction the average electric field can be expressed as,

$$|E(x, y, z)|^2 = E_0^2 \frac{w_0^2}{w(z)^2} \exp\frac{-2(x^2 + y^2)}{w(z)^2} \quad (5)$$

where  $w(z) = w_0 \left(1 + (\frac{z}{z_R})^2\right)^{\frac{1}{2}}$  and  $E_0$  is the electric field amplitude. Here  $w_0$  is the beam waist at the focus, and  $z_R$  is the Rayleigh length. By carrying out a series expansion around  $x = y = z = 0$  and discarding terms of third order and higher, a harmonic approximation of the potential is obtained,

$$U(x, y, z) = U_0 \left( \frac{2(x^2 + y^2)}{w_0^2} + \frac{z^2}{z_R^2} \right) \quad (6)$$

where  $U_0 = -\frac{1}{2}\alpha_g E_0^2$ . The oscillation frequencies in the three directions are  $\omega_x^2 = \omega_y^2 \simeq 4U_0/mw_0^2$ ,  $\omega_z^2 \simeq 2U_0/mz_R^2$ . When the total laser power is shared with a second beam propagating in the  $x$  direction which crosses the first beam at its focus, these frequencies change to  $\omega_y^2 \simeq 4U_0/mw_0^2$ ,  $\omega_x^2 = \omega_z^2 \simeq 2U_0/mw_0^2$  at the intersection point. This assumes that the beams have identical properties and  $z_R \gg w_0$ . According to these results, an abrupt change from a two beam to a one beam geometry will produce a significant frequency change along the  $z$  direction. The ratio of one and two beam frequencies is,

$$\frac{\omega_{1\text{beam}}}{\omega_{2\text{beam}}} = \frac{w_0}{z_R} = \frac{\lambda}{\pi w_0} \quad (7)$$

which is independent of the total laser power and is determined by the beam waist at the focus. Since the temperature of the atomic cloud is proportional to the momentum

distribution squared, combining Eqs. (3) and (7) gives

$$\frac{T_{\text{final}}}{T_{\text{initial}}} = \left(\frac{\omega_1}{\omega_0}\right)^2 = \left(\frac{\lambda}{\pi w_0}\right)^2. \quad (8)$$

To explore this behavior experimentally we aligned the CO<sub>2</sub> beams such that their foci overlapped. Atoms were loaded into the potential minimum created by the intensity maximum located at the intersection of the beams. The power in the  $x$  beam was transferred to the  $z$  beam by switching the RF power on the second AOM to zero. This abrupt transfer of power mostly produced a change in the effective frequency in the  $z$  direction and initiated the oscillation of the trapped cloud. If the shift of power to the  $z$  beam happens immediately after loading, the FORT will not produce the desired oscillation since the atomic density is approximately  $10^{14}$  atoms cm<sup>-3</sup> and cold binary scattering dramatically affects the evolution of the cloud. Therefore the collisionless approximation of the previous section can not be used. To move into the collisionless regime it is necessary to decrease the atomic density by reducing the number of atoms before the power transfer. This is accomplished by reducing the total power in the CO<sub>2</sub> beams in order to carry out forced evaporation of hot atoms. This reduces both the density of atoms in the trap and their temperature. This process is carried out so that the atomic cloud which remains in the FORT has densities of around  $10^{11}$  atoms cm<sup>-3</sup>. This guarantees that the mean free path of the individual particles is bigger than the cloud size so that the evolution of the sample can be considered in the collisionless regime.

After evaporative cooling the total power was transferred to the  $z$  beam and the cloud size started to oscillate in the  $z$  direction. However, the time evolution of the cloud size did not obey the simple periodic form predicted by Eq. (2). Our observations show that a domain with high atomic density appears at the center of the trap periodically during the cloud's evolution. This structure is reminiscent of the two component structure which appears at the onset of a degenerate Bose gas. Three cross sections of the cloud along the  $z$ -axis are shown in Fig.1. Figure1 (a), (b) and (c) were taken 2, 5 and 10 ms after switching off the  $x$  beam respectively. The total power in the CO<sub>2</sub> beams was 5 Watts. A high density region at the center of Fig. 1(b) is clearly visible. It disappears later in the evolution as seen in Fig. 1(c). Creation of these high density regions is a direct result of the strong anharmonic potential and is predicted in [13]. A Monte Carlo simulation of the anharmonic system can reproduce this behavior for the cloud. Figure 2 presents the result of such a collisionless

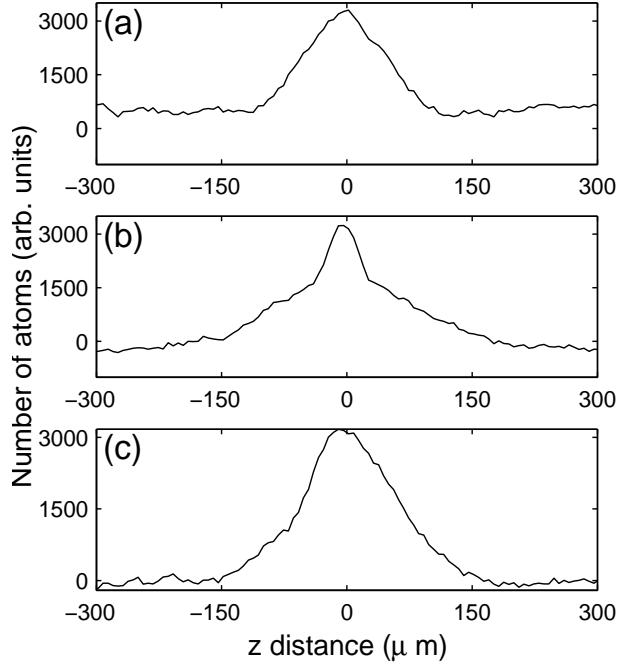


FIG. 1: The accumulated intensity along the  $x$ -axis as a function of  $z$  distance. Two beams from a  $\text{CO}_2$  laser crossed each other at right angles with overlapping foci and 5 Watts power. (a), (b) and (c) were obtained 2, 5 and 10 ms after extinguishing the  $x$  beam. A denser component is obvious at the center of the cloud in (b).

calculation at the moment where the two component structure appears. The simulation was carried out for  $3 \times 10^4$  atoms initially at thermal equilibrium with a  $25\mu\text{m}$  initial cloud size. It is worth noting that the high density regions never appeared when harmonic potentials were simulated.

The high density region makes the observed optical density profiles complex enough that it is impossible to fit a Gaussian function to the data and infer the width of the cloud. Therefore to observe the oscillation of the cloud size, predicted by Eq. (2) we have reduced the total power in the  $\text{CO}_2$  beams to 0.5 Watts. In this regime the cloud temperature is low enough (below  $2 \mu\text{K}$ ) that the oscillation amplitude does not move the atoms away from the region where the harmonic approximation of the potential is valid. Furthermore, as mentioned above, the evaporative cooling also reduces the atomic density to  $\approx 10^{11}$  atom  $\text{cm}^{-3}$ , suppressing the two-body collision rate. The time dependency of the cloud size for this condition is given in Fig. 3. This shows that the cloud does not collapse to its original

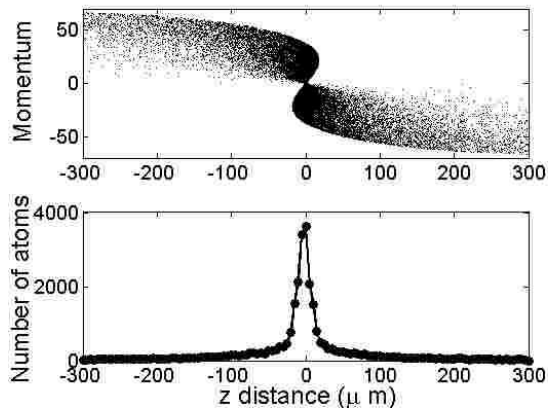


FIG. 2: (a) Calculated  $z$  direction phase space distribution of the atoms at the moment where the two component structure appears. The atoms were initially distributed uniformly throughout the phase space and physically located at the cross over of two beams with overlapping foci. The horizontal axis is the  $z$ -direction spread of the particles in units of the beam waist and the vertical axis is the  $z$ -momentum in units of the photon recoil from a 780 nm photon. (b) The corresponding histogram of the particles' distribution in the  $z$  direction.

extent during its evolution in the trap. We expect that this is the result of a small number of collisions. According to this data the size of the cloud in the  $z$  direction expands to about 6 times its initial value. From Eq. (3) this implies a factor of 6 reduction in the width of the momentum distribution or a factor of 36 in the effective  $z$ -direction temperature. This number in combination with Eq. (8) determines the beam waist at  $\approx 20\mu\text{m}$ , in good agreement with the theoretically calculated value of  $\approx 23\mu\text{m}$ .

#### IV. MOVING CENTER OF MASS

In contrast to most other work with FORTs, we also studied geometries where the center of mass moves as a result of a change in the potential. This was achieved by offsetting the foci of the  $\text{CO}_2$  beams from each other. In this configuration, when one of the beams was switched off, the atoms moved towards the new potential minimum located at the focus of the remaining beam. For a harmonic trap the center of mass and internal dynamics of the atomic cloud are decoupled from one another. However, for an anharmonic trap the periodic motion of the center of mass of the atoms couples to the internal dynamics. Figure

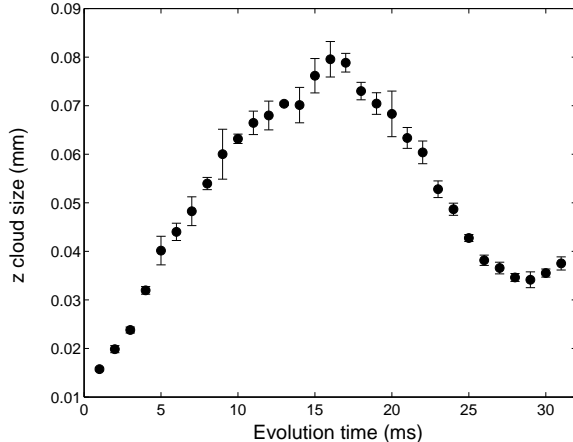


FIG. 3: Evolution of the  $z$  cloud size inside the  $z$  beam for a stationary center of mass. Two beams from a  $\text{CO}_2$  laser crossed each other at right angles with overlapped foci. The power in the  $x$  beam was abruptly transferred to the  $z$  beam at  $t=0$  to initiate the cloud's oscillation.

4 schematically displays the trapping potential before and after power is transferred to the  $z$  beam.

The observed  $z$  cloud size as a function of time for one period is presented in Fig. 5. As occurred in the previous section, the cloud size in this direction never shrinks to its initial value. Figure 5 also shows that the cloud undergoes a considerable increase in width by the time it reaches the focus of the  $z$ -beam at  $t \approx 10\text{ms}$ . It can be seen that the cloud size increases by as much as 10 times its initial value. This implies a compression in momentum spread by a similar factor and thus we expect a two order of magnitude reduction of the effective temperature in the  $z$ -direction. This is significantly more than was possible in the stationary center of mass experiments.

We also performed experiments in which the potential was switched off completely after the atoms had evolved for various times inside the  $z$ -beam. There are several features of the cloud's evolution after release from the  $z$ -beam that are worthy of note. Firstly, it is possible to tune the center of mass velocity in the  $z$ -direction with high precision. This can be accomplished by changing the time span that the cloud evolves inside the  $z$ -beam before it is switched off. Such a property could be useful for quantum reflection experiments where precise control of the impact velocity is required [23]. A second aspect of the free evolution is the observation of a collapse of the cloud in the  $z$ -direction during the first

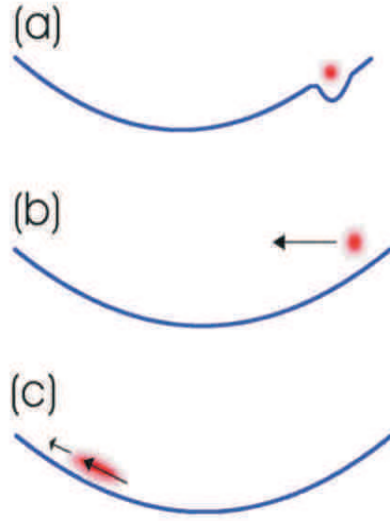


FIG. 4: Schematic of the dipole potential (a) before and (b) after transferring the power of the  $x$  beam to the  $z$  beam. In (b) the center of mass of the atomic cloud oscillates around the Gaussian focus of the remaining light. (c) cloud size after evolving inside the  $z$  beam for approximately half a period. The difference in velocities at the two ends of the cloud gives rise to a collapse after the potential is switched off for a TOF experiment

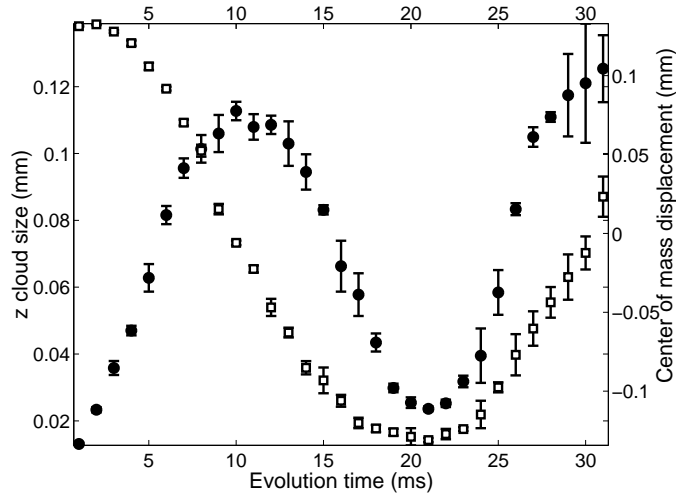


FIG. 5: The cloud size (closed circles) and center of mass position (open squares) in the  $z$  direction while evolving inside the  $z$  beam. Initially two beams from a  $\text{CO}_2$  crossed each other at right angles with their foci displaced by  $\approx 140 \mu\text{m}$ . The power in the  $x$  beam was abruptly transferred to the  $z$  beam at  $t=0$ .

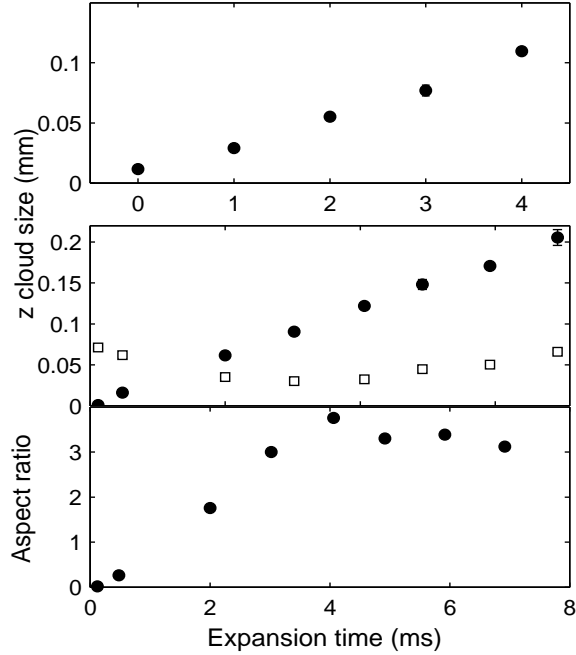


FIG. 6: Experimental data showing the cloud size. The power was 5 Watts per  $\text{CO}_2$  beam. The circular and square symbols represent the cloud size in the  $x$  and  $z$  directions respectively. (a) shows the results after various expansion times for the case where the FORT has been directly released from the crossed beams. Note that the circle and square symbols overlap each other in this case. In (b) the  $x$  and  $z$  cloud sizes are shown for the condition where the power from the  $x$  beam was switched to the  $z$  beam 15 ms before releasing the FORT. In (c) the ratio of the  $x$  to  $z$  cloud sizes of (b) is presented.

few milliseconds after the atoms are released. To observe this collapse the cloud is first allowed to evolve inside the  $z$ -beam for nearly half a period of the center of mass motion. The collapse can be explained by the velocity difference between the atoms on either side of the cloud imprinted by the gradient of the trapping potential. This can be seen in Fig. 4(c). The exact time at which to switch the  $z$ -beam off to observe the maximum collapse is determined experimentally. This time is 16 ms for the experiment shown in Fig. 5. The resulting collapse or focusing can be used to transfer energy from the  $z$  to the  $x$  and  $y$  directions if the cloud has high enough densities such that the free expansion starts when the cloud is in the collisional regime. Under this condition, since at the release time the trap has become elongated in the  $z$  direction, the atoms moving along the  $z$  direction experience

a larger number of collisions compared to the  $x$  and  $y$  directions and part of their  $z$  kinetic energy transfers into  $x$  and  $y$  while expanding [24]. To explore this possibility, unlike in the previous section, the evaporative cooling is carried out such that the cloud had a density of  $\approx 10^{14}$  atoms  $\text{cm}^{-3}$  (this corresponds to a mean free path of  $9\mu\text{m}$  for our system). The velocity distribution should remain constant with time after the expansion makes the mean free path larger than the cloud size and the atoms reach the collisionless regime. Therefore to determine the temperature the asymptotic expansion rate of the cloud data must be used [25] after it has reached the collisionless regime .

For comparison we have conducted another series of experiments in which the power in the  $\text{CO}_2$  laser was switched off without transferring total power to the  $z$  beam. Figure 6(a) shows the size of the atomic cloud as a function of time after release from a crossed beam trap with 5 Watts of power. As can be seen, the expansion of the atoms is isotropic ( $x$  and  $z$  data overlap) and the corresponding temperature is about  $3.7(2) \mu\text{K}$ . In Fig. 6(b) the cloud size as a function of time is given for an experiment in which the atoms were released from the crossed beam trap (off-set foci) and then allowed to evolve for 6 ms inside the  $z$  beam before all potentials were switched off and the free expansion began. The asymptotic velocity for the elongated trap extracted from data given in Fig. 6(b) gives  $T_z = 0.43(2) \mu\text{K}$  and  $T_x = 4.4(2) \mu\text{K}$ . The higher temperature in the  $x$  direction is caused by the focusing of the cloud and the extra collisions atoms undergo in the  $z$  direction because of the compressed cloud. The ratio is  $T_x/T_z = 10.2$  which is quite close to the square of the mean aspect ratio = 3.3 for the collisionless expansion. Figure 6(c) shows the ratio of the  $x$  to  $z$  size of the cloud at different times. Figure 7 shows the atomic cloud's image for 4 different times during the free expansion. Figure 7(a) shows the cloud at the crossed beam without expansion and Fig. 7(b) is the same cloud after 4 ms free expansion. Fig. 7(c) is taken 6 ms after turning the vertical beam off and Fig. 7(d) is the same cloud after 4 ms of free expansion. The accurate simulation of the individual atomic trajectories for the free expansion is very time consuming because of the two-body cold collisions. In order to overcome this problem we employ the direct simulation Monte Carlo (DSMC) method which was initially developed by Bird [26] to simulate molecular gas dynamics. This method has been used for direct simulation of evaporative cooling [27] and free expansion of the cloud of atoms [24]. Using this method the behavior of a cloud of atoms with  $2 \mu\text{K}$  temperature initially displaced  $0.5z_R$  from the potential minimum created by a gaussian beam with 25

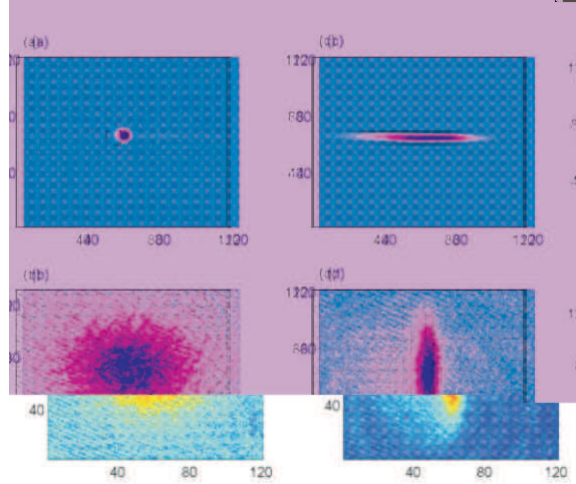


FIG. 7: Images of the atomic cloud. (a) shows cloud at the beginning of the time of flight released from two crossed beams. In (b) the same cloud after 4 ms free expansion. (c) released from the crossed beam FORT 6 ms after turning off the  $x$  beam and (d) is the same cloud imaged 4 ms after the  $x$  beam has been extinguished. Each pixel in the images is  $6 \times 6 \mu\text{m}$ .

$\mu\text{m}$  beam waist was simulated. Figure 8 shows the simulated momentum distribution in the  $z$  (narrow distribution) and  $x$  (broad distribution) directions after 5 ms free expansion. The initial density was taken  $1.8 \times 10^{14} \text{ atom cm}^{-3}$ . As one can see the axial distribution deviates little from a perfect gaussian. This has been reported previously for an expanding cloud [24].

## V. CONCLUSION

In this paper we have studied the effect of geometrical changes of the trap on the atomic cloud evolution. We experimented with two configurations of crossed laser beams. In the first set of experiments, the foci of two orthogonal beams were positioned to coincide. The foci of the beams were subsequently offset for the second set of experiments. In each case, the behavior of the cloud upon abruptly switching off the  $x$  beam was studied. In the overlapped foci experiment we observed high atomic density domains, due to the strong anharmonic trapping potential. To reach the collisionless regime the trap density was reduced by lowering the power in the beams. We observed oscillations in the axial  $z$  direction with an amplitude up to a factor of 6 times the original cloud size. This implies that the momentum had been

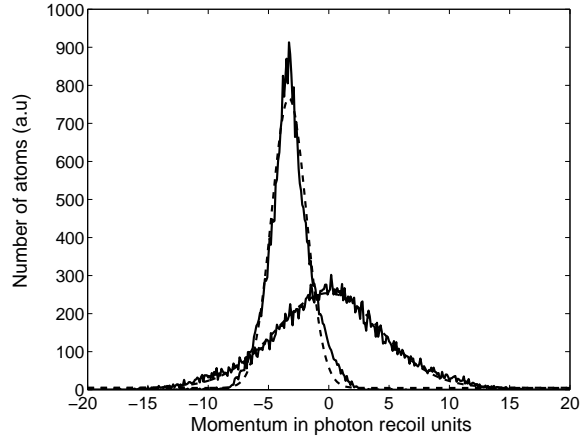


FIG. 8: Simulated momentum distributions in  $z$  and  $x$  directions after 5 ms free expansion. Broken lines are the gaussian fit to the data. The narrow and broad curves are the  $z$  and  $x$  distributions respectively.

reduced by a factor of 36. When the beams' foci were offset, cloud sizes as much as 10 times the initial cloud size were achieved. In this later case we observed the atomic cloud to collapse in the  $z$  direction when released from certain positions in the trap. An energy transfer from the  $z$  to the  $x$  direction was observed for this release condition for clouds with high densities.

Considering the fact that the cloud's center of mass gains a  $z$  velocity this system could be a useful tool in the study of quantum reflection of cold atoms from material surfaces [28, 29, 30]. Another possible avenue for further investigations would be subjecting a Bose-Einstein condensate to these potentials.

P. Ahmadi was supported by an Oklahoma EPSCoR Nanonet grant and B.P. Timmons was supported by a NASA Space Grant Fellowship.

- 
- [1] Stamper-Kurn D M, Miesner H -J, Chikkatur A P, Inouye S, Stenger J and Ketterle W 1998 *Phys. Rev. Lett.* **81**, 2194.
  - [2] Stamper-Kurn D M, Miesner H -J, Inouye S, Andrews M R and Ketterle W 1998 *Phys. Rev. Lett.* **81**, 500.
  - [3] Rudy P, Ejnisman R and Bigelow N P 1997 *Phys. Rev. Lett.* **78**, 4906.

- [4] Raithel G, Birkl G, Phillips W D and Rolston S L 1997 *Phys. Rev. Lett.* **78**, 2928.
- [5] Janszky J, Yushin Y Y 1986 *opt. Commun.* **59**, 151.
- [6] Janszky J, Adam P 1989 *Phys. Rev. A.* **39**, 5445.
- [7] Aliga J, grespo G and Proto N 1990 *Phys. Rev. A.* **42**, 618.
- [8] Lo C F 1990 *J. Phys. A* **23**, 1155.
- [9] Agarwal G S and Kumar S A 1991 *Phys. Rev. Lett.* **67**, 3665.
- [10] Janszky J, Yushin Y 1992 *Phys. Rev. A.* **46**, 6091.
- [11] Leibscher M and Averbukh I Sh 2002 *Phys. Rev. A.* **65**, 053816.
- [12] Balatov A, Vugmeister B, Burin A and Rabitz H 1998 *Phys. Rev. A.* **58**, 1346.
- [13] Balatov A, Vugmeister B and Rabitz H 1999 *Phys. Rev. A.* **60**, 4875.
- [14] Flories M H Crompvoets *et al.* 2002 *Phys. Rev. Lett.* **89**, 093004.
- [15] Ketterle W *et al.* 2003 *Science*, **301**, 1513.
- [16] Hubert Ammann and Nelson Christensen 1997 *Phys. Rev. Lett.* **78**, 2088.
- [17] Barrett M D, Sauer J A and Chapman M S 2001 *Phys. Rev. Lett.* **87**, 010404.
- [18] Görlitz A, Weidemüller M, Hänsch T W and Hemmerich A 1997 *Phys. Rev. Lett.* **78**, 2096.
- [19] Rudy R, Ejnisman R and Bigelow N P 1997 *Phys. Rev. Lett.* **78**, 4906.
- [20] Monroe C 1997 *Nature (London)* **388**, 719.
- [21] Ahmadi P, Timmons B P, Summy G S 2005 *Phys. Rev. A.* **72**, 023411.
- [22] Ahmadi P, Ramareddy V, Summy G S 2005 *New Journal of Physics*, **5**, 7.
- [23] Japha Y and Band Y B 2002 *J. Phys. B: At. Mol. Opt. Phys.* **35** 2383.
- [24] Wu H, Arimondo E 1998 *Europhys. Lett.* **43**, 141.
- [25] Shvarchuk I *et al.* 2003 *Phys. Rev. A.* **68**, 063603.
- [26] Bird G A, 1994 *Molecular Gas Dynamics and the Direct Simulation of Gas Flow* (Oxford:Clarendon).
- [27] Wu H, Foot C J 1996 *J. Physics. B.* **29**, L321.
- [28] Anderson A *et al.* 1986 *Phys. Rev. A.* **34**, 3513.
- [29] Berkhout J J *et al.* 1989 *Phys. Rev. Lett.* **63**, 1689.
- [30] Shimizu F 2001 *Phys. Rev. Lett.* **86**, 987.